CoMFA Model of Anti-tumor Activity for Fluoroquinolon-3-yl s-Triazole Sulfide-ketone Derivatives and Implications for Molecular Design①

CHEN Kui-Qing FENG Chang-Jun②

(*School of Chemistry & Chemical Engineering, Xuzhou University of Technology, Xuzhou* 221018, *China*)

ABSTRACT Comparative molecular field analysis (CoMFA) techniques were used to perform three-dimensional quantitative structure-activity relationship (3*D*-QSAR) studies on the anti-tumor activity (pI_H and pI_C) of 28 fluoroquinolon-3-yl s-triazole sulfide-ketone derivatives (FQTSDs) against two cancer cell lines, including human hepatoma Hep-3B cells and human pancreatic cancer Capan-1 cells. 23 compounds were randomly selected as the training set to establish the prediction models, which were verified by the test set of 6 compounds containing template molecule. The obtained cross-validation (R_{cv}^2) and non-cross-validation correlation coefficients (R^2) of the CoMFA models were 0.477 and 0.850 for pI_H, and 0.421 and 0.836 for pI_C, respectively. The contributions of steric and electrostatic fields to pI_H were determined to be 48.1% and 51.9%, and those to pI_C were 49.4% and 50.6%, respectively. The CoMFA models were then used to predict the activities of the compounds in the training and testing sets, and the models had a strong stability and good predictability. Based on the 3*D* contour maps, four novel FQTSDs with a higher anti-tumor activity were designed. However, the effectiveness of these novel FQTSDs is still needed to be verified by experimental results.

Keywords: fluoroquinolon-3-yl s-triazole sulfide-ketone derivative, **anti-tumor activity**, **3*D*-QSAR**, **comparative molecular field analysis**, **molecular design; DOI: 10.14102/j.cnki.0254–5861. 2011–3000**

1 INTRODUCTION

Fluoroquinolone antibiotics are a class of drugs commonly used by people and animals. Because of the broad-spectrum antibacterial property, strong antibacterial activity, no cross-resistance with other antibacterial drugs and little toxic and side effects, they are widely used in animal husbandry, aquatic products and other aquaculture industries. Since topoisomerase (Topo), the antibacterial target of fluoroquinolones, is also an important target of anti-tumor drugs, the antibacterial activity of fluoroquinolones can be regarded as anti-tumor activity[1, 2].

It is the most economical and reliable strategy in the research and development of new drugs to modify the structure of existing drugs to obtain lead compounds with the potential to be developed into powerful drugs[3]. Among various strategies, rational drug molecular design based on the substitution of bioelectronic isoelectric isomer of pharmacophore and the combination of pharmacophore is a common method in the construction of new drug molecules[4]. The structural modification of fluoroquinolones showed that C-3 carboxyl group was a pharmacophore necessary for antibacterial activity but not for anti-tumor activity, and the antibacterial activity can be transformed into anti-tumor activity by the substitution of heterocycles or condensed heterocycles[5].

In this context, much research work has been conducted on the design of anti-tumor fluoroquinolone molecules. Ni et al.[6] designed and synthesized 14 fluoroquinolone C-3 s-triazole thioether ketone derivatives by splicing effective pharmacophore or shifting dominant drug skeleton. Meanwhile, Xie et al.[7] designed and synthesized 14 fluoroquinolone C-3 s-triazole thioether ketone derivatives by using s-triazole as C3 carboxyl iso-isomer of antibacterial fluoroquinolones, based on the bioelectronic iso-isomer design principle of pharmacophore. These 28 compounds are collectively called fluoroquinolon-3-yl s-triazole sulfide-ketone derivatives (FQTSDs). The authors[6, 7] further evalua-

Received 12 October 2020; accepted 26 November 2020

① This project was supported by the National Natural Science Foundation of China (21075138) and special fund of State Key Laboratory of Structural Chemistry (2016028)

② Corresponding author. Feng Chang-Jun, male, born in 1954, professor, majoring in quantitative structure-activity correlation researchship. E-mail: fengcj@xzit.edu.cn

ted the anti-tumor activities of these FQTSDs to human hepatoma Hep-3B cells and human pancreatic cancer Capan-1 cells (expressed as "IC_{50}", unit: μmol dm^{-3}) by the methyl thiazolyl tetrazolium (MTT) assay, with doxorubicin as the positive control drug.

Quantitative structure-activity relationship (QSAR) plays an important role in predicting the biological activity of compounds and is becoming increasingly important in the field of chemistry, medicine, environment and other disciplines[8-13]. The research methods of QSAR mainly include two-dimensional QSAR (2*D*-QSAR) and three-dimensional QSAR (3*D*-QSAR) methods[14-17]. The major difference is that 3*D*-QSAR methods incorporate the three-dimensional conformational properties of bioactive molecules. Therefore, they can reflect the real images of interactions between bioactive molecules and receptors more accurately, and reveal the mechanisms of drug-receptor interactions more deeply. Moreover, the fitting results of 3*D*-QSAR are generally better than 2*D*-QSAR. In recent years, 3*D*-QSAR methods have been applied extensively in correlating chemical structure features with biological activities to obtain some basis information for further compound design and synthesis. Especially, the comparative molecular field analysis (CoMFA)[14-17] is a widely used 3*D*-QSAR method that establishes relationships between the biological activity of drug molecules and their steric and electrostatic fields. The Van Der Waals potentials and Coulomb potentials, which represent steric and electrostatic fields, respectively, can be calculated by the standard Tripos force field with the Gasteiger-Hückel charges.

In this study, we aim to establish 3*D*-QSAR models of the anti-tumor activity[6, 7] of FQTSDs against two tumor cell lines (Hep-3B and Capan-1) by CoMFA method. According to the established model, the key structural features affecting anti-tumor activity were revealed, and novel molecules with a higher anti-tumor activity were further designed for future potential applications.

2 MATERIALS AND METHODS

2. 1 Studied compounds and their anti-tumor activity data

28 FQTSDs[6, 7] were tested for cytotoxic activity (IC_{50}, Half maximal inhibitory concentration) against two tumor cell lines (Hep-3B and Capan-1) by in *vitro* MTT assay. The IC_{50} for Hep-3B and Capan-1 are denoted by "I_H" and "I_C ", respectively. The basic structures of these compounds are shown in Fig. 1, with the corresponding substituents Ar and the I_H and I_C data listed in Table 1.

Table 1. Experimental and Predicted pI_H and pI_C Values of FQTSDs Using the CoMFA Models

No.	Ar	I_H[6, 7]	I_C[6, 7]	p$I_{H.exp.}$	p$I_{H.cal.}$	p$I_{C.exp.}$	p$I_{C.cal.}$
1	Ph	27.3	15.3	4.564	4.580	4.816	4.821
2*	4-CH_3O-Ph	31.7	18.6	4.499	4.398	4.731	4.612
3	4-OH-Ph	28.5	16.4	4.545	4.461	4.785	4.677
4	4-CH_3-Ph	45.6	23.4	4.341	4.268	4.631	4.457
5	4-F-Ph	12.8	8.6	4.893	4.868	5.066	5.183
6	4-Cl-Ph	33.4	17.4	4.477	4.710	4.760	5.006
7	4-NO_2-Ph	15.3	8.2	4.816	4.769	5.086	5.064
8*	Ph	17.6	10.5	4.755	4.692	4.979	5.013
9	4-CH_3O-Ph	18.3	8.7	4.738	4.742	5.061	5.060
10	4-OH-Ph	16.4	7.5	4.785	4.803	5.125	5.168
11	4-CH_3-Ph	26.8	13.6	4.572	4.561	4.867	4.817
12	4-F-Ph	7.4	2.3	5.131	5.014	5.638	5.443
13	4-Cl-Ph	15.6	7.5	4.807	4.940	5.125	5.346
14	4-NO_2-Ph	6.7	2.0	5.174	5.133	5.699	5.623
15*	Ph	36.7	28.6	4.436	4.628	4.544	4.732
16	4-CH_3O-Ph	38.4	31.2	4.416	4.460	4.506	4.548
17	4-CH_3-Ph	41.6	38.7	4.381	4.321	4.413	4.384
18	4-Cl-Ph	21.3	16.4	4.672	4.678	4.785	4.827
19	4-Br-Ph	23.5	15.2	4.629	4.620	4.818	4.767
20	4-F-Ph	12.6	7.2	4.900	4.896	5.143	5.072
21*	4-NO_2-Ph	8.5	5.1	5.071	4.767	5.293	4.924
22	Ph	25.4	18.5	4.595	4.622	4.733	4.771

To be continued

23	4-CH_3O-Ph	27.5	21.6	4.561	4.634	4.666	4.772
24	4-CH_3-Ph	28.3	25.4	4.548	4.462	4.595	4.509
25	4-Cl-Ph	15.2	10.3	4.818	4.916	4.987	5.143
26	4-Br-Ph	17.6	12.7	4.755	4.908	4.896	5.132
27*	4-F-Ph	4.7	3.2	5.328	4.971	5.495	5.218
28	4-NO_2-Ph	4.3	1.5	5.367	5.117	5.824	5.435
29	4-SO_3H-Ph				5.185		5.531
30	4-SO_2NH_2-Ph				5.094		5.421
31	4-CO_2H-Ph				5.369		5.803
32	4-CO_2CH_3-Ph				5.138		5.448

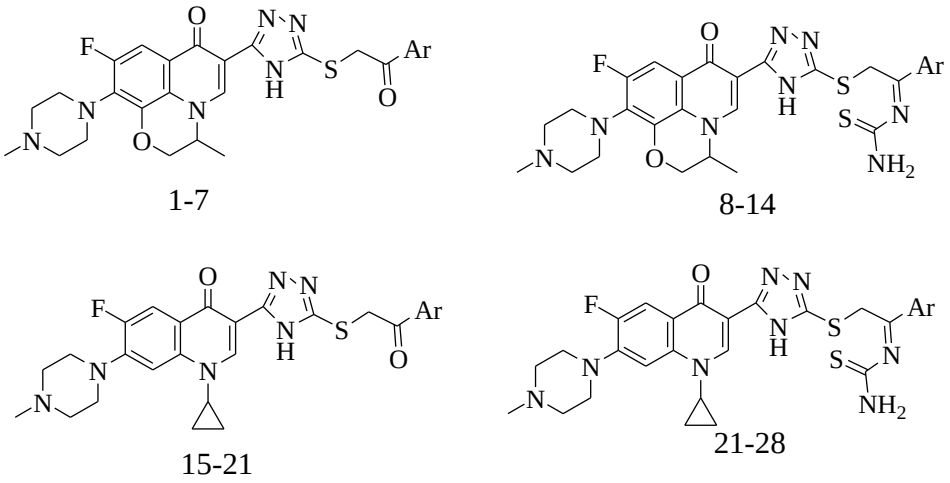

Fig. 1. Basic structures of FQTSDs

According to the equilibrium principle of physical chemistry, there is a logarithmic relationship between free energy change (ΔGr) and concentration (c)[18]. Therefore, by taking the negative logarithm of IC_{50} (pIC = –logIC_{50}), all initial anti-tumor activity (I_H and I_C) values[6, 7] are converted into pI_H and pI_C to be used as dependent variables in CoMFA research. The pI_H and pI_C values of the 28 FQTSDs are also shown in Table 1. The data set was randomly divided into a training set of 23 compounds for model generation and a test set of 6 compounds (including template molecule, marked with "*" in Table 1) for model validation.

2. 2 Molecular modeling and alignment

All molecular modeling and calculations for CoMFA[19-22] were carried out by Sybyl package (Latest version Sybyl-x2.1.1, Tripos Inc., St. Louis, MO, USA) on a LINUX RH6.4/WIN7 64BIT/WIN864BIT/MAC operating system. The energy minimization was performed using the Tripos force field with a distance-dependent dielectric function and Powell conjugate gradient algorithm with a convergence criterion of 0.005 kcal/(mol·Å), and the number of iterations was 1000. Partial atomic charges were calculated using the Gastieger-Huckel method. The remaining parameters used in CoMFA were all default unless otherwise stated. Structural alignment is considered as one of the most sensitive parameters in CoMFA analysis. The accuracy of the prediction of CoMFA model and the reliability of contour maps are directly dependent on the structural alignment rule. The most active compound, *i.e.*, No. 28 for Hep-3B and Capan-1, was selected as the template for the molecular alignment.

The common substructures of these molecules, which are composed of the non-hydrogen atoms, are shown in Fig. 2. Each analog was aligned to the template by rotation and translation using the DATABASE ALIGNMENT command in Sybyl so as to minimize root mean square deviation (RMSD) between atoms in the template and the corresponding atoms in the analog. These alignments were subsequently used in calculations of CoMFA probe interaction energy. The alignment results based on the above strategies are shown in Fig. 3.

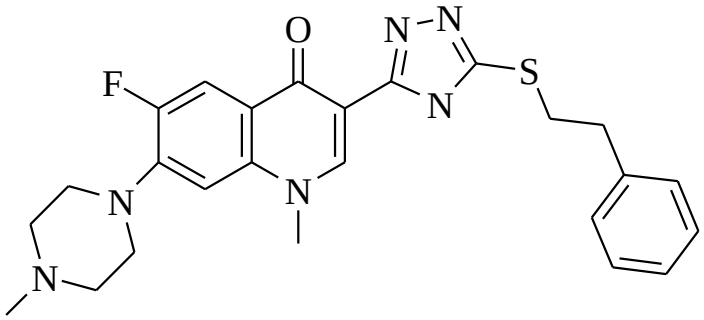

Fig. 2. Common substructure of the molecules employed for molecule alignment

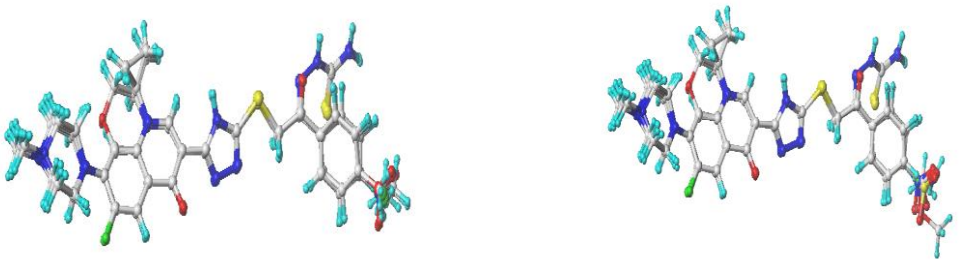

(a) **(b)**

Fig. 3. 3*D* view of all the aligned molecules in the training set (a) and test set (b)

2. 3 Model generation and validation

CoMFA fields, which were the interaction energies between a probe atom or a molecule and a set of aligned molecules, are used to establish the 3*D*-QSAR model. The steric and electrostatic contributions were truncated at 30 kcal/mol, and electrostatic contributions were dropped at lattice intersections with maximum steric interaction.

Partial least-squares (PLS) analysis was used to construct a linear correlation between the 3*D*-fields (independent variables) and the anti-tumor activity values (pI_H and pI_C, as dependent variables) of FQTSDs. First of all, leave-one-out cross-validation method was used to determine the cross-validation correlation coefficients (R_{cv}^2) and the optimal number (N) of components. Generally, when R_{cv}^2 is greater than > 0.3, the established model is statistically significant at the significance level of 5%, *i.e.*, the reliability of the model is 95%[23]. Moreover, the model is required to have a *S*v (The ratio of compound number (m) to variable number (n)) of $\geqslant$ 5 has statistical significance and low probability[24]. In addition, non-cross-validation method was also used to further assess the robustness and statistical confidence of the derived models. According to the general statistical standard, a value of $R^2 \geqslant 0.80$ indicates that the model fitting is good[25].

3 RESULTS AND DISCUSSION

3. 1 The established 3*D*-QSAR models

Based on the CoMFA method, the 3*D*-QSAR models of the anti-tumor activity of FQTSDs on two kinds of cells were constructed, and the results are shown in Table 2, where N is the optimal component number, R_{cv}^2 the cross-validation correlation coefficient, R^2 the non-cross-validation correlation coefficient, *SD* the estimated standard error, *F* the Fisher value, and St. and El. represent the contribution rates of stereo and electrostatic fields, respectively.

3. 2 Quality evaluation of the 3*D*-QSAR models

(1) Cross-validation: The R_{cv}^2 of the two models is both greater than 0.3 (Table 2), which indicates that they have good prediction ability and robustness. Furthermore, it meets the current preferred standard of $R_{cv}^2 > 0.4$[26]. The *S*v equals to 5.75 (*S*v = 23/4), larger than 5, indicating that the models are statistically significant.

Table 2. Fitting Results of the CoMFA Models for pI_H and pI_C

Cell	*N*	R_{cv}^2	R^2	*F*	*SD*	St. (%)	El. (%)
Hep-3B	4	0.477	0.850	25.561	0.110	48.1	51.9
Capan-1	4	0.421	0.836	22.988	0.163	49.4	50.6

(2) Non-cross-validation: The R^2 is both greater than 0.8 (Table 2), suggesting the two models have good correlation and stability. Thus, over 83.6% of the change of anti-tumor activity can be explained by field energy of FQTSDs, and only less than 16.4% is attributed to a random factor. At the significant level of 95%, the critical value of statistical variance ratio (F) is $F_{0.05}$ (4,18) = 2.93[27]. The F value of these two models is obviously greater than 2.93, suggesting that the relationship between dependent and independent variables is very significant.

Then, the calculated values (for the training set) and predicted values (for the test set) for pI_H and pI_C of FQTSDs are obtained by using these two CoMFA models. These values are very close to the corresponding experimental data (the minimum deviation for pI_H is 0.357, and the deviation for pI_C is less than 0.389, see Table 1 and Fig. 4 for specific data). All statistical parameters show that the models generated from CoMFA method are reasonable and have good predictability.

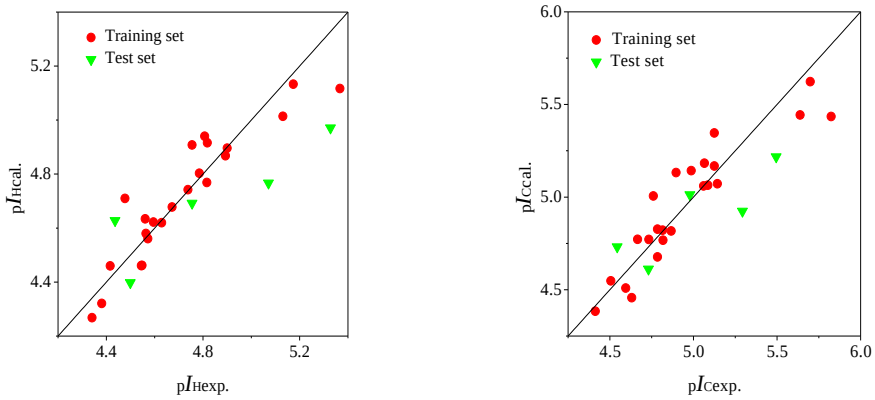

Fig. 4. Scatter plots of the experimental versus predicted pI_H and pI_C values of FQTSDs

(3) Field energy contribution: The steric and electrostatic contributions were found to be close to 48.8% and 50.8%, respectively. Electrostatic field has a slightly greater influence than the steric field, which indicates that the electrostatic interaction of ligands may be a slightly more important influencing factor of anti-tumor activity.

3. 3 Main factors affecting the anti-tumor activity from a combined CoMFA analysis

The results of CoMFA can be displayed as vivid 3*D* contour maps of steric and electrostatic fields, providing an effective way to explain the observed variance in the anticancer activity (expressed as pI_H and pI_C). CoMFA steric map is represented by green and yellow contours: green contours indicate the regions where the existence of bulky group would be favorable for anticancer activity, while yellow contours represent regions where bulky group would decrease the activity. In the electrostatic field map, blue and red contours denote the regions that the anticancer activity would be increased by the presence of electron-donating and electron-withdrawing groups, respectively.

3. 3. 1 Steric contour maps

Fig. 5 shows the steric contour maps for the CoMFA models of pI_H and pI_C with the most active molecule 28 as a reference. In the contour map, two models are very similar. The spatial distribution of the stereo field shows that the introduction of a larger group at the 4-position (green region) of the benzene ring and the presence of two smaller groups at the distant 3,5-position (yellow region) of the benzene ring are both conducive to improving the anti-tumor activity. For example, when the group at the 4-position of benzene ring is -NO_2 group, the pI_H and pI_C are generally larger (Table 1: Nos. 7, 14, 21 and 28. Especially, the Nos. 14, 21 and 28 molecules have the largest activity value in the same group of compounds.).

3. 3. 2 Electrostatic contour maps

Fig. 6 shows the electrostatic contour maps for the CoMFA models of pI_H and pI_C with the most active compound 28 as a reference. The two figures are also very similar, which have two smaller blue regions near and on the 4-position of benzene ring, a larger red region far away from the 4-position, and a slender blue region at thiosemicarbazone. For the compounds containing thiosemicarbazone (No. 8～14 and 22～28), the H atoms with partial positive charge in thiosemicarbazone is in the blue region, so their anti-tumor activities are stronger than those of compounds No. 1～7 and 15～21. The electron-withdrawing ability of F, Cl and Br

decreased in sequence, and thus the positive electricity of the neighboring 4-carbon atom in the halogenated FQTSDs was decreased correspondingly, leading to a decline in the anti-tumor activity, just as the case of No. 27 > 25 > 26. The anti-tumor activity of the compounds with 4-NO_2 group is almost the strongest in the same class, because the two negative oxygen atoms are located in the red region, while the positive nitrogen atoms in the blue region. This further verified the findings of Ni et al.[6] and Xie et al.[7] that the electron-withdrawing groups (such as F and N) in the benzene ring and the introduction of thiosemicarbazone can significantly enhance the anti-tumor activity.

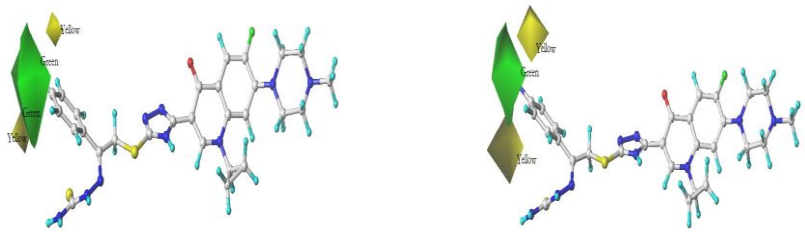

pI_H **pI_C**

Fig. 5. CoMFA steric contour maps with compound 28 as a reference

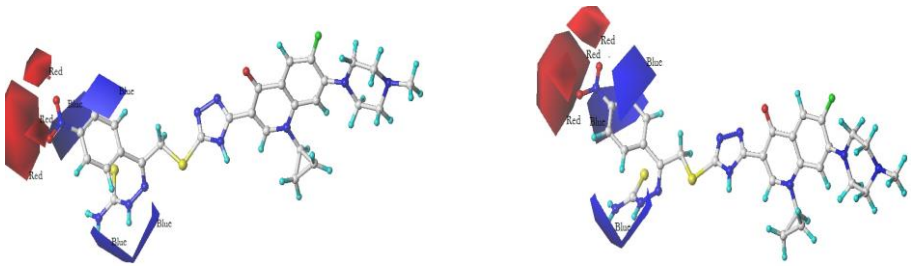

pI_H **pI_C**

Fig. 6. CoMFA electrostatic field contour maps with compound 28 as a reference

3. 3 Theoretical design of new FQTSDs with higher anti-tumor activity

One of the purposes of QSAR research is to design molecules from the structural information implied in the established model and to predict the biological activity of the designed molecules by the model, providing theoretical basis for the synthesis of new highly active molecules. It can be seen from the above discussions on the spatial distribution of electrostatic and stereo fields that the introduction of a group similar to nitro group at the 4-position of benzene ring is conductive to improving anti-tumor activity. According to this rule, four new compounds were designed (Table 1, compounds 29～32), and their pI_H and pI_C values were further predicted by the two 3*D*-QSAR models. For most of these compounds, they have even better anti-tumor activity than the most effective drugs reported in the literature. To be specific, the anti-tumor activity of molecules 29, 31 and 32 is stronger than that of template molecule (No. 28) due to the fact that the electronegativity of nitrogen atom is greater than that of sulfur and carbon atoms, and these atoms are located in the blue region. However, it should be pointed out that the anti-tumor activity of No. 30 molecule is weaker than that of template molecule because the connection of electron-donating NH_2 group reduces the positive charge on the sulfur atom. Despite of the theoretically high anti-tumor activity, these new FQTSDs need to be further verified by biomedical experiments.

4 CONCLUSION

(1) The CoMFA method was applied to systematically study the anti-tumor activities (pI_H and pI_C) of a series of FQTSDs against two cancer cell lines, including human hepatoma Hep-3B cells and human pancreatic cancer Capan-1 cells. The established CoMFA models showed good fitting and high predictive ability in terms of large correlation coefficient (pI_H: R^2 = 0.850, pI_C: R^2 = 0.836) and cross-validation correlation coefficient (pI_H: R_{cv}^2 = 0.477, pI_C: R_{cv}^2 = 0.421).

(2) The two CoMFA models give some insights into the mechanism of the anti-tumor effects of FQTSDs: (a) The action mechanism of FQTSDs on Hep-3B and Capan-1 tumor cells is very similar; (b) The contribution of electrostatic effect is close to that of stereo effect; (c) When the 4-position

of benzene ring is introduced with a group similar to nitro structure, the anti-tumor activity will be greatly enhanced.

(3) According to the established 3*D*-QSAR models, four novel FQTSDs with excellent anti-tumor activity are designed, which needs to be further verified by biomedical experiments.

This work is the first attempt to successfully establish two CoMFA models of anti-tumor activity for FQTSDs, and the information obtained in this study would provide helpful theoretical information for predicting the anticancer activities of related novel FQTSDs derivatives and guiding the synthesis of new potent anticancer drugs through structural modifications.

REFERENCES

(1) Mayer, C.; Janin, Y. L. Non-quinolone inhibitors of bacterial type IIA topoisomerases: a feat of bioisosterism. *Chem. Rev*. **2014**, 114, 2313−2342.

(2) Zhou, Y.; Xu, X.; Sun, Y.; Wang, H. P.; Sun, H. P.; You, Q. D. Synthesis, cytotoxicity and topoisomerase II inhibitory activity of lomefloxacin derivatives. *Bioorg. Med. Chem. Lett.* **2013**, 23, 2974−2978.

(3) Pirhadi, S.; Shiri, F.; Ghasemi, J. B. Methods and applications of structure-based pharmacophores in drug discovery. *Curr. Top. Med. Chem.* **2013**, 13, 1036−1047.

(4) Guo, Z. R. Strategy of molecular drug design: activity and druggability. *Acta Pharm. Sin.* **2010**, 45, 539−547.

(5) Gao, L. Z.; Xie, Y. S.; Li, T.; Huang, W. T.; Hu, G. Q. Synthesis, antitumor activity and SAR of C-3 oxadiazole sulfanylacetylhydrazone-substituted fluoroquinolone analogues. *Acta Pharm. Sin.* **2014**, 49, 1694−1698.

(6) Ni, L. L.; Yan, Q.; Wu, S. M.; Xie, Y. S.; Gao, L. Z.; Liu, Y. J.; Huang, W. L.; Hu, G. Q. Synthesis and antitumor activity of fluoroquinolon-3-yl-s-triazole sulfide ketones and their derivatives from ciprofloxacin. *Acta Pharm. Sin*. **2015**, 50, 1258−1262.

(7) Xie, Y. S.; Gao, L. Z.; Yan, Q.; Wu, S. M.; Ni, L. L.; Liu, Y. J.; Huang, W. L.; Hu, G. Q. Synthesis and antitumor activity of fluoroquinolon-3-yl s-triazole sulfide-ketone thiosemicarbazone derivatives of ofloxacin. *Chin. J. Appl. Chem.* **2016**, 33, 25−31.

(8) Abdulla, A. M.; Mei, Z.; Qiu, L.; Ju, X. H. Theoretical investigation on QSAR of (2-methyl-3-biphenylyl) methanol analogs as PD-L1 inhibitor. *Chin. J. Chem. Phys.* **2020**, 33, 459−467.

(9) Zheng, S. S.; Li, T. T.; Wang, J.; Hu, Y. J.; Zhang, H. X.; Zhao, S. X.; Zhao, Y. H.; Li, C. QSAR models for predicting the aqueous reaction rate constants of aromatic compounds with hydrated electrons. *Envir. Chem.* **2019**, 38, 1005−1013.

(10) Yang, F.; Wang, M.; Wang, Z. Y. Sorption behavior of 17 phthalic acid esters on three soils: effects of p*H* and dissolved organic matter, sorption coefficient measurement and QSPR study. *Chemosphere* **2013**, 93, 82−89.

(11) Qu, R. J.; Liu, H. X.; Feng, M. B.; Yang, X.; Wang, Z. Y. Investigation on intramolecular hydrogen bond and some thermodynamic properties of polyhydroxylated anthraquinones. *J. Chem. Engin. Data* **2012**, 57, 2442−2455.

(12) Zeng, X. L.; Qu, R. J.; Feng, M. B.; Chen, J.; Wang, L. S.; Wang, Z. Y. Photodegradation of polyfluorinated dibenzo-*p*-dioxins (PFDDs) in organic solvents: experimental and theoretical studies. *Environ. Sci. Technol*. **2016**, 50, 8128−8134.

(13) Qu, R. J.; Liu, J. Q.; Li, C. G.; Wang, L. S.; Wang, Z. Y.; Wu, J. C. Experimental and theoretical insights into the photochemical decomposition of environmentally persistent perfluorocarboxylic acids. *Water Research* **2016**, 104, 34−43.

(14) Feng, H.; Du, X. H.; Chen, Y.; Feng, C. J. 3*D*-QSAR models of anti-tumor activity for histone deacetylase inhibitors containing dihydropyridin-2-one. *Chin. J. Struct. Chem.* **2020**, 39, 855−862.

(15) Tong, J. B.; Qin, S. S.; Lei, S.; Wang, Y. A 3*D*-QSAR study of HIV-1 integrase inhibitors using RASMS and Topomer CoMFA. *Chin. J. Struct. Chem.* **2019**, 38, 867−881.

(16) Shu, M.; Wu, T.; Wang, B. W.; Li, J.; Xu, C. M.; Lin, Z. H. 3*D*-QSAR and surflex docking studies of a series of alkaline phosphatase inhibitors. *Chin. J. Struct. Chem.* **2019**, 38, 7−16.

(17) An, C. H.; Shu, M.; Zai, X. L.; Zhang, B. N.; Li, J.; Chang, Z. C.; Hu, Y.; Lin, Z. H. Combined 3*D*-QSAR, pharmacophore and docking studies on benzene-sulfonamide derivatives as potent 12-lipoxygenase inhibitors. *Lett. Drug Des. Discov*. **2017**, 14, 74−82.

(18) Guo, Z. R. *Molecular Drug Design*. Science press. Beijing **2005**, p20.

(19) Feng, C. J. CoMFA model of herbicidal activity of phenyl-sulfonylured derivatives. *J. Xuzhou Inst. Tech.* (*Nat. Sci. Ed.*) **2019**, 34, 21−25.

(20) Feng, C. J. CoMFA model of inhibitory activity for nitrobenzene derivatives to photobacteria. *J. Xuzhou Inst. Tech.* (*Nat. Sci. Ed.*) **2020**, 35, 28−31.

(21) Joshi, S. D.; More, U. A.; Aminabhavi, T. M.; Badiger, A. M. Two- and three-dimensional QSAR studies on a set of antimycobacterial pyrroles: CoMFA, Topomer CoMFA, and HQSAR. *Med. Chem. Res.* **2014**, 23, 107−126.

(22) Cramer, R. D.; Patterson, D. E,; Bunce, J. D. Comparative molecular field analysis (CoMFA). 1. Effect of shape on binding of steroids to carrier proteins. *J. Am. Chem. Soc.* **1988**, 110, 5959−5967.

(23) Hu, S. Q.; Mi, S. Q.; Jia, X. L.; Guo, A. L.; Chen, S. H.; Zhang, J.; Liu, X. Y. 3D-QSAR study and molecular design of benzimidazole derivatives as corrosion inhibitors. *Chem. J. Chin. Univ.* **2011**, 32, 2402−2409.

(24) Liu, D.; Zhang, W.; Xu, L. Quantitative structure-activity/property relationships for chiral hydroxy acids and amino acids. *Acta Chim. Sin.* **2009**, 67, 145−150.

(25) Zhang, J.; Shen, P.; Lu, T.; Yu, D.; Li, H.; Yang, G. Theoretical studies on quantitative structure-activity relationship and structural modification for the inhibition of MMP-9 by flavonoids. *Acta Chim. Sin.* **2011**, **69**, 383−392.

(26) Anshuman, D.; Sushil, K. K.; Stuti, G.; Anil, K. S. Development of CoMFA, advance CoMFA and CoMSIA models in pyrroloquinazolines as thrombin receptor antagonist. *Bioorg. Medic. Chem.* **2004**, 12, 3591−3598.

(27) Sun, W. S.; Chen, L. C. *Statistics* (Second edition). China agricultural university press. Beijing **2012**, p241, 242, 470.